Journal of Power Sources 197 (2012) 267–275

Contents lists available at SciVerse ScienceDirect

Journal of Power Sources

journal homepage: www.elsevier.com/locate/jpowsour

Long lifetime in concentrated LiOH aqueous solution of air electrode protected with interpenetrating polymer network membrane

Fouad Ghamouss, Mohamed Mallouki, Bruno Bertolotti, Linda Chikh, Cédric Vancaeyzeele, Séverine Alfonsi, Odile Fichet*

Laboratoire de Physicochimie des Polymères et des Interfaces (LPPI – EA 2528) – Université de Cergy-Pontoise – 5, mail Gay-Lussac, 95031 Cergy-Pontoise Cedex, France

ARTICLE INFO

Article history:
Received 24 July 2011
Received in revised form
14 September 2011
Accepted 16 September 2011
Available online 22 September 2011

Keywords:
Interpenetrating polymer network
Anionic membrane
Air electrode
Discharge stability

ABSTRACT

Solid anion-exchange membranes that display interpenetrating polymer network (IPN) architecture were developed to be assembled on air electrode surface to improve its electrochemical stability in alkaline environment. The IPN membranes associate an anionic conducting polyepichlorohydrin network entangled within a cross-linked poly(2-hydroxyethyl methacrylate) in different mass proportions. The membranes possess suitable mechanical and thermal properties, an ionic conductivity of about 1×10^{-3} S cm^{-1} and suitable cation selectivity. The electrochemical behaviour of the air electrode/IPN membrane assemblies (AEMA) were then evaluated in LiOH 5 M. The polarization curves indicate that a good electrochemical interface was established between the electrode and the IPN membranes. Moreover, the AEMA exhibits a discharge stability in LiOH 5 M ten times higher compared to a bare electrode under the same conditions.

1. Introduction

Air electrodes are widely used as positive electrodes in energy conversion and storage systems such as fuel cells and metal/air batteries. It is usually a three-layer structure composed of a porous support layer, a hydrophobic gas diffusion layer and a porous active layer [1]. The special feature of this kind of electrode is that the active component, i.e. oxygen, is not stored in the electrode material but comes from air during the discharge process. The capacity of an air electrode is therefore considered as unlimited. Furthermore, alkaline electrolyte, such as an aqueous hydroxide salt, is used in some batteries because it leads to an increase of the kinetic reaction and permits the use of cheaper catalysts based on non-noble metals in the active layer of air electrode [2,3]. However, technical locks persist for the development of such an energy storage system. Indeed, air electrodes show a limited lifetime in alkaline environment. Several degradation mechanisms have been proposed [4–7]. The reaction between carbon dioxide contained in atmospheric air and the liquid alkaline electrolyte (LiOH, NaOH, KOH, etc.) leading to carbonate formation constitutes a major hindrance [8,9]. Indeed, insoluble carbonate formed inside the air electrode structure destroys the porous structure leading to the electrochemical activity decrease [10]. In addition, the diminution of both OH^- concentration and oxygen solubility results in a decrease of the anodic and cathodic reaction rates, respectively. The most common way to avoid the deleterious influence of carbon dioxide is simply to remove it by using commercial CO_2 air scrubbers [1]. But the use of this strategy depresses the interest of metal–air battery systems coming from their high specific energy since only the negative active mass must be stored in the battery.

Under atmospheric air, one potential solution to ensure a better electrochemical stability of the air electrode in alkaline environment is to protect the electrode with a polymer membrane. This membrane must ensure the required hydroxide conduction for the electrochemical reactions performing at the electrode and it must also prevent the transport of cationic species (K^+, Li^+, Zn^{2+}, etc.) from the electrolyte towards the triple phase boundary where the carbonate formation occurs. Under these conditions, the reaction is drastically reduced inside the air electrode structure. Therefore, research has focused on the development of solid anion-exchange membranes with cationic functions on the polymer backbone to ensure anionic conduction. Only a few cationic membranes were evaluated as solid polymer electrolytes for alkaline fuel cells. The most common anion exchange membranes were achieved by chemical grafting of ionic conducting sites onto polymer chains that include quaternized and cross-linked poly(vinylbenzyl chloride) [11,12], methyl pyridinium-immobilized poly(vinyl alcohol) [13], quaternized-chitosan [14,15], polysulfone matrix [16–18], polysulfonium [19], quaternized poly(ether ether ketone) [20] or polyether [21]. Fauvarque et al. have developed a series of cationic membranes based on polyepichlorohydrin (PECH) [22–25]. The polymer was cross-linked by nucleophilic substitution (SN2) of

* Corresponding author. Tel.: +33 134257050; fax: +33 134257071.
E-mail address: odile.fichet@u-cergy.fr (O. Fichet).

0378-7753/$ – see front matter © 2011 Elsevier B.V. All rights reserved.
doi:10.1016/j.jpowsour.2011.09.052

cyclic diamine such as 1,4-diazabicyclo-[2,2,2]-octane (DABCO) onto the chlorine of polyepichlorohydrin. In such electrolytes, the cationic sites are quaternary ammonium groups that exhibit a higher thermal and chemical stability compared to other quaternary cations such as quaternary phosphonium or tertiary sulfonium groups [26]. Furthermore, this cyclic quaternary ammonium group does not undergo Hoffman degradation in alkaline medium [27].

Cross-linking density of the network can be increased by using a poly(epichlorohydrin-allyl glycidyl ether) copolymer in which the allyl groups are cross-linked via a thiol-ene addition [28,29]. These membranes are very attractive due to their thermal and chemical stabilities. However, the single PECH network is brittle and exhibits a high electrolyte swelling ratio which causes a loss in its dimensional stability. A polyamide support is thus necessary in order to improve the mechanical strength of these PECH based membranes. The intrinsic conductivity of the polyamide supported PECH membrane was found to be low (10^{-4}–10^{-5} S cm^{-1}). The polyamide support was suspected to decrease the membrane–water affinity as well as ionic mobility [25].

Another promising strategy that could improve the mechanical properties of a cationic PECH based membrane consists in including a PECH network into interpenetrating polymer network (IPN) architecture. IPNs were defined by Sperling as the combination of two or more polymer networks synthesized in juxtaposition [30,31]. The entanglement of two cross-linked polymers into the IPN leads to forced miscibility of usually incompatible polymer blends, and the resulting materials exhibit a good dimensional stability. The purpose of this type of polymer associations is generally to combine each partner's properties inside a homogenous material while their flaws are cancelled. Even if this last point cannot be considered as being always true, specific applications of these materials have been carried out thanks to improved solvent resistance and mechanical properties of different objects, in vibration and noise damping, controlled release of drugs or other reactive compounds [32–35]. This architecture has been also used for the synthesis of fuel cell membrane [36].

Few studies have reported the synthesis of PECH-based IPNs [37–39]. In these cases, PECH network was synthesized starting from a hydroxyl-terminated polyepichlorohydrin and a pluriisocyanate cross-linker via an alcohol–isocyanate addition leading to a urethane group formation. This PECH network has been associated with a polymethyl(meth-)acrylate or polyethyl(meth-)acrylate networks in order to obtain a reinforced elastomer by adjusting the IPN weight composition. All the IPNs with various compositions have a single Tg (measured by DSC) which corresponds to only one mechanical relaxation detected by DMTA measurements. Both partner networks are thus compatible as confirmed by TEM microscopy where no phase separation was detected. The tensile strength of the IPNs is enhanced several times compared with that of PECH network with little decrease of elongation. Thus the PECH network mechanical properties can be improved when included inside an IPN architecture, but PECH network is not used as a polyelectrolyte in these different cases.

The present paper describes the synthesis of a new IPN anion conducting membrane, which can protect an air electrode in alkaline environment. These membranes were first synthesized according to an *in situ* process in which polyepichlorohydrin and poly(2-hydroxyethyl methacrylate) (PHEMA) networks were combined in different weight compositions. These two polymers are respectively responsible for the anionic conductivity and the mechanical properties. The mechanical and thermal properties of membranes were characterized by dynamic mechanical thermal analysis (DMTA) and thermo gravimetric analysis (TGA), respectively. The ionic conductivity and transport number were also determined. Finally, the electrochemical characteristics of commercial air electrodes, modified and not by these IPN membranes, were studied by chronopotentiometric technique. Finally, the life times of IPN modified air electrodes, operating in concentrated aqueous lithium hydroxide under untreated air, were evaluated. The carbonate precipitation is fast in the lithium hydroxide solutions under air atmosphere (Li_2CO_3 solubility in water is lower at 20 °C (13 g L^{-1}) compared with that of K_2CO_3 (1120 g L^{-1}) [41]). In addition, lithium hydroxide has been chosen as electrolyte because the corresponding air electrode aims at being part of a Li/air battery.

2. Experimental

2.1. Materials

Polyepichlorohydrin (PECH) modified with 0.12 equiv. 1,4-diazabicyclo-[2,2,2]-octane (DABCO) was purchased as ethanol/butanone (80/20 wt%) solution (100 g L^{-1}) from ERAS Labo (France). This solution was previously concentrated to 130 g L^{-1} under reduced pressure at room temperature. 2-Hydroxyethyl methacrylate (HEMA – Aldrich), ethylene glycol dimethacrylate (EGDMA cross-linker – Aldrich), potassium hydroxide (KOH >90% – Aldrich), and lithium hydroxide (LiOH 98% – Acros) were used without further purification. Free-radical initiator 2,2′-azobisisobutyronitrile (AIBN – Aldrich) was recrystallized in methanol before use. Deionized water was used for electrolyte solution preparation and ionic exchange process.

The air electrode (E5 Electric Fuel®), purchased from Electric Fuel, is composed of a porous polytetrafluorethylene film combined with a cobalt based catalyzed carbon supported on a metal mesh.

2.2. Membranes synthesis

2.2.1. PHEMA membrane

Single PHEMA network was synthesized by mixing 0.9 g HEMA, 0.1 g EGDMA and 0.05 g AIBN (5 wt% of monomers). Then the mixture was degassed under argon for 15 min and poured into a mould made from two glass plates clamped together and sealed with a 250 μm thick Teflon® gasket. The mould was heated at 60 °C for 16 h and transparent PHEMA material was obtained.

2.2.2. PECH membrane

Single PECH network was synthesized by pouring 5 mL PECH solution into a Petri dish (7.2 cm diameter). The Petri dish was heated at 100 °C for 4 h. A 100 μm homogeneous and transparent PECH film was obtained.

2.2.3. IPN membranes

All the IPNs were synthesized according to an *in situ* process. For example, PECH/PHEMA IPN in 37/63 wt% was prepared by mixing 0.60 g HEMA and 0.06 g EGDMA in 3 mL PECH solution (130 g L^{-1}). The mixture was stirred for 30 min under argon. AIBN (5 wt% with respect to methacrylate compounds) was then dissolved in the mixture. The homogenous mixture was poured into a mould made from two glass plates clamped together and sealed with a 250 μm thick Teflon® gasket. The mould was placed in an oven at 60 °C for 16 h and at 100 °C for 2 h. Finally the transparent PECH/PHEMA IPN film was demolded at room temperature.

IPNs with different PECH contents ranging from 37 to 90 wt% were synthesized by keeping the same proportions between monomer, cross-linker and initiator for PHEMA network. All the films were synthesized from 3 mL PECH solution (130 g L^{-1}) in which different HEMA weights were added. All investigated PECH/PHEMA compositions are reported in weight ratio.

2.2.4. Semi-IPNs membranes

Semi-IPNs (IPN in which one of the polymers is linear) were synthesized according to the same synthesis pathway as the IPNs.

In one case EGDMA was not added to the reaction mixture in order to obtain semi-IPNs in which PHEMA is linear. In a second case the semi-IPNs in which PECH is linear were obtained by suppressing the second step at 100 °C of the cure program (necessary for the PECH cross-linking reaction).

2.3. Characterizations

All samples were dried up to constant weight under vacuum (5 mmHg) at 50 °C for at least 3 days before characterization.

2.3.1. Soluble fractions (SF)

Soluble fractions (uncross-linked components) contained in the different single networks, semi-IPNs and IPNs were quantified from a known weight of dry material (W_0) extracted in a Soxhlet with DMF for 48 h. After extraction, the samples were dried under vacuum at 50 °C until constant weight (W_E). The soluble fraction (SF) was calculated as a weight ratio:

$$\text{SF}\ \ (\%) = \frac{W_0 - W_E}{W_0} \times 100$$

2.3.2. Water uptake (Wu)

Water uptake was determined by measuring the weight difference of the materials before and after immersion in deionized water at room temperature for 48 h (i.e. to equilibrium). The samples were removed from water, wiped rapidly with filter paper and weighed (W_w). Then the wet sample was subsequently dried at 60 °C under vacuum until constant weight (W_d). The water uptake was calculated as:

$$\text{Wu}\ \ (\%) = \frac{W_w - W_d}{W_d} \times 100$$

2.3.3. Spectroscopy impedance

Ionic conductivity was measured by electrochemical impedance spectroscopy using an Autolab PGSTAT 30 Instrument. The samples were put between two platinized blocking electrodes. Nyquist plots were recorded with a Frequency Response Analysis (FRA) over frequency range of 200 kHz to 1 Hz with oscillation amplitude of 30 mV. The ionic conductivity was then calculated using the relation

$$\sigma = \frac{l}{R \times S},$$

where l and S denote the thickness and the surface of the material between two electrodes, respectively. The electrical resistance (R) was measured from the intercept of the Nyquist plot at high frequency with the real impedance axis. Intrinsic conductivity was measured on water swollen samples. The hydroxide conductivity was measured on samples in which chloride ions were previously exchanged with hydroxide ones. To achieve this exchange, a sample was immersed in 1 mol L^{-1} KOH aqueous solution for 24 h. The sample was then rinsed several times with deionized water and finally immersed in a large volume of water for one day in order to remove the KOH excess.

2.3.4. Transport number

The membrane transport numbers under diffusion were determined according to a static method derived from Henderson's equation previously described [25]. The membrane separates the cell in two compartments each containing KOH solutions with concentrations of 0.1 and 1 mol L^{-1}. The voltage measured between two Hg/HgO electrodes immerged in each compartment is the sum of the electromotive force ($\Delta\varphi$) and of the membrane potential ($\Delta\varphi_M$). As $(t^+ + t^-) = 1$, the anionic transport number was determined from the following relation [40]:

$$t^- = \frac{1}{2}\left[1 + \frac{F}{RT}\frac{\Delta\varphi_M}{\ln(a_{\text{KOH,1 M}}/a_{\text{KOH,0.1 M}})}\right]$$

where F is Faraday constant, R is gas constant, T is temperature, and a the activities of different KOH solutions.

2.3.5. Mechanical analysis

Dynamic mechanical thermal analysis (DMTA) was carried out with a Q800 model (TA instruments) operating in tensile mode at 1 Hz frequency. Strain magnitude was set at 0.05% of the sample length, value ensuring that the tests were made in the linear viscoelastic domain. Temperature varied from −100 to 160 °C with heating rate of 3 °C min^{-1}. The set up provides the storage and loss moduli (E', E'') and the loss factor ($\tan\delta = E''/E'$).

Rheological measurements were performed with an Anton Paar Physica MCR 301 rheometer equipped with CTD 450 temperature control device with plate–plate (diameter 25 mm) geometry. All measurements were recorded at an imposed 0.2% deformation at 1 Hz frequency at 25 °C on samples that were previously fully hydrated by immersion in water for 48 h. The average value of the shear modulus was measured for 5 samples.

2.3.6. Thermo gravimetric analysis (TGA)

TGA measurements were carried out with a Q50 model (TA instruments) under argon atmosphere operating from room temperature to 600 °C with a 20 °C min^{-1} heating rate. The degradation temperatures were measured at 5% weight loss of the sample.

2.3.7. Electrochemical characterization

The air electrode/membrane assembly (AEMA) was prepared by pressing at 3 bar for 30 s a wet polymer membrane (100–150 μm) on the catalyst-coated electrode surface. Then, the AEMA was placed between two Teflon® plates which were pressed at 3 bar at 60 °C for 30 min.

Air electrode/membrane assembly was mainly characterized by electrochemical experiments, performing in a conventional three-electrode in-house constructed half-cell. Air electrode with geometric area of 3.8 cm^2 was used as working electrode. Hg/HgO/1 mol L^{-1} KOH electrode was used as reference, and large area platinized titanium grid as counter electrode. A 5 mol L^{-1} LiOH aqueous solution was used as alkaline electrolyte. All measurements were carried out at ambient temperature and under atmospheric pressure with untreated air. The half-cells were equilibrated in 5 mol L^{-1} LiOH electrolyte solution for 1 h before starting the chronopotentiometric measurements to obtain the potential versus current density curves.

Stability of the air electrodes, modified or not with a membrane, was evaluated from the air electrode potential–time curves recorded when the half-cells were cycled using a 10 h polarization step (−10 mA cm^{-2} current density) followed by 10 h at open circuit voltage (OCV).

3. Results and discussion

3.1. Membrane synthesis

The anionic conductivity of the membrane can be ensured by an appropriate cross-linked polyelectrolyte. However polyelectrolyte networks show an important swelling in aqueous electrolyte solution such that a low selectivity towards cations is observed. In order to limit swelling, the polyelectrolyte can be associated with a neutral polymer in an interpenetrating polymer network (IPN) architecture [30,31] to obtain self-supported polyelectrolyte based

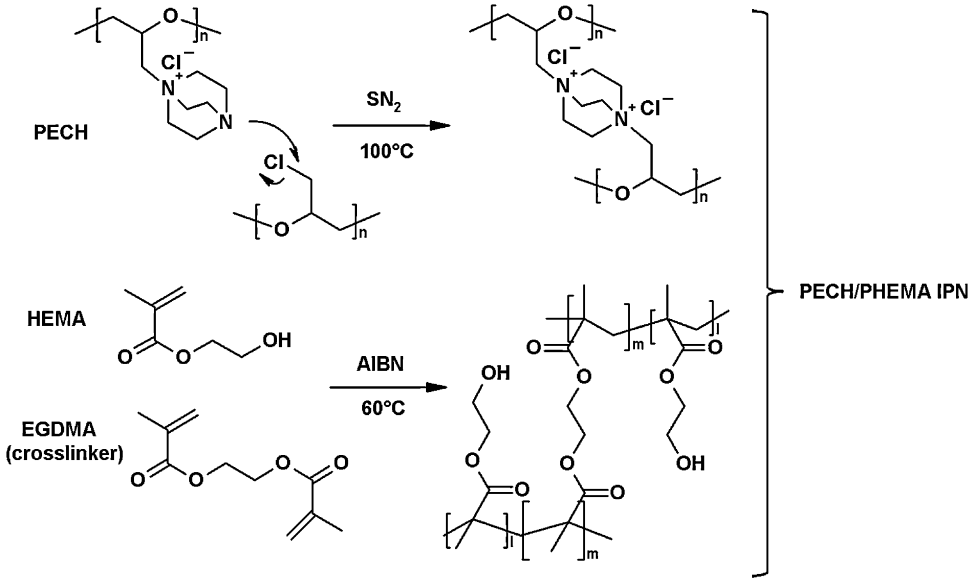

Scheme 1. PECH/PHEMA interpenetrating polymer networks synthesis.

homogeneous materials. These IPN membranes are synthesized according to an *in situ* process (all compounds are mixed before the cross-linking reactions).

As shown in Scheme 1, polyepichlorhydrin (PECH) was chosen as the polyelectrolyte precursor. This elastomer shows a glass transition temperature of −21 °C [42], which guarantees a good flexibility and should facilitate ionic conduction. The poly(oxyethylene) skeleton with hanging CH_2–Cl groups on each monomer unit allows the incorporation of quaternary ammonium functions by nucleophilic substitution by amines such as 1,4-diazabicyclo-[2,2,2]-octane (DABCO). This reaction occurs at temperatures higher than 80 °C, thus it was carried out at 100 °C in this study. The cross-link loci are also the cationic sites which will ensure the ionic conductivity of the material.

The PECH is combined with poly(2-hydroxyethyl methacrylate) (PHEMA) network as a neutral polymer to provide mechanical stability and limited water swelling. PHEMA network is synthesized through a free-radical copolymerization of 2-hydroxyethyl methacrylate (HEMA) monomer with ethylene glycol dimethacrylate (EGDMA) as cross-linker (Scheme 1). This reaction is initiated with AIBN at 60 °C. Thus, the PHEMA network can be considered as first formed at 60 °C and then the PECH network is formed at 100 °C during the IPN synthesis. All the IPNs are homogeneous and transparent and they are further characterized.

To check that no grafting reaction occurs between both networks during the IPN synthesis, two kinds of PECH/PHEMA (67/33) semi-IPNs were synthesized. If no grafting reaction occurs, the linear polymer can be extracted quantitatively from a semi-IPN by Soxhlet extraction. A semi-IPN in which linear PHEMA is entrapped in PECH network is prepared by omitting EGDMA in the reaction mixture. As expected, the soluble fraction in DMF is equal to 32 wt%. The soluble fraction has been identified by ^{13}C NMR as linear PHEMA. This result shows that no grafting reaction occurred between the two polymers. To obtain a semi-IPN in which PECH is not cross-linked in the material, the PECH cross-linking step at 100 °C is avoided. In this case, the soluble fraction in DMF is equal to 47 wt% instead of the expected 62 wt%. The soluble fraction was identified by ^{13}C NMR as linear PECH. This result suggests that the PECH modified with DABCO can partially cross-link at 60 °C. In order to check this assumption, linear PECH non modified with DABCO was used for the synthesis of a third semi-IPN in which only PHEMA is cross-linked, the step at 100 °C being maintained. In this case, the soluble fraction in DMF is equal to 72 wt% confirming that linear PECH can be extracted from PHEMA network. As the linear polymers can be quantitatively extracted from semi-IPNs, no side reaction occurs between the network precursors. The synthesized materials can be then qualified as IPNs.

Table 1
Soluble fractions contained in single PECH and PHEMA networks and IPNs.

PECH/PHEMA IPN (w/w)	Soluble fraction (wt%)
0/100 (PHEMA network)	8
(37/63)	7
(43/57)	6
(50/50)	7
(67/33)	5
100/0 (PECH network)	6

To further check that cross-linking reactions are completed, the amount of soluble fraction contained in the different networks and IPNs is determined by Soxhlet extraction with DMF. All the soluble fractions are lower than 8 wt% (Table 1). For example, the PECH/PHEMA 67/33 IPN contains 5 wt% of soluble fraction, identified by ^{1}H NMR as being linear PECH and PHEMA, which confirms the correct cross-linking of these polymers. Thus, PECH and PHEMA networks are correctly cross-linked inside the IPN architecture.

3.2. Characterizations of PECH based IPNs

It is also important to verify that the PECH based IPNs show suitable mechanical properties, i.e. they are easy to handle and show a significant resistance such that they can be pressed on the surface of air electrode without breaking nor perforating. Thus, storage modulus (E') and loss factor ($\tan\delta$) of the single networks and IPNs are measured by DMTA (Fig. 1).

Single PECH network displays a glassy plateau (E' = 900 MPa) at temperatures lower than −10 °C (Fig. 1(A)). Above this temperature, the storage modulus values decrease sharply and a rubbery plateau is reached at 50 °C (E' = 2 MPa). PHEMA network shows also a single mechanical relaxation versus temperature. The glassy plateau extends up to 50 °C and the rubbery plateau is reached at 130 °C at E' = 10 MPa. IPNs show a higher storage modulus than single PECH network whatever the IPN composition. Thus PECH network association with a thermoplastic network as PHEMA inside an IPN architecture leads to an improvement of the storage

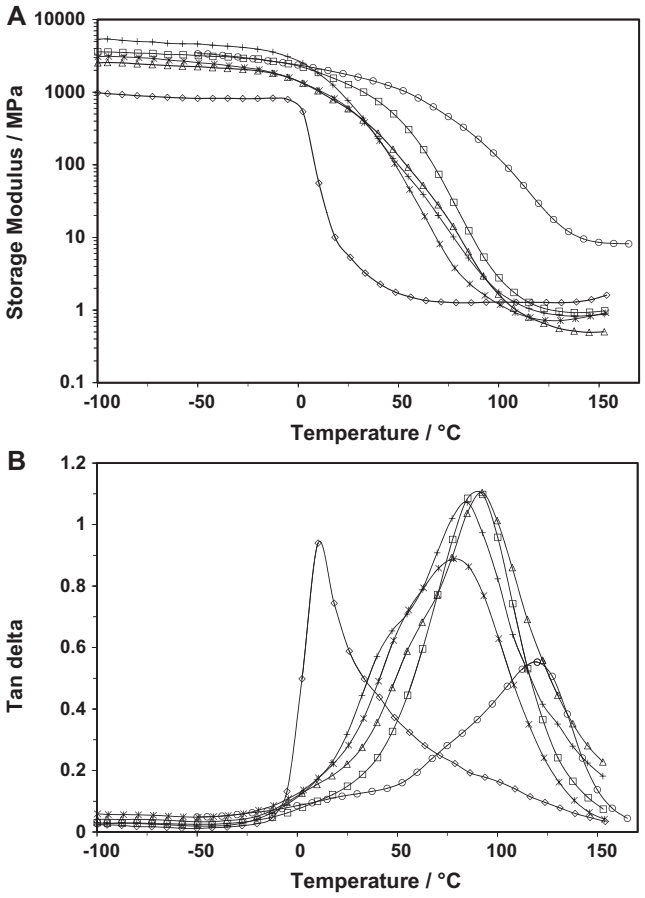

Fig. 1. (A) Storage modulus (E') and (B) tan δ versus temperature of single PECH (◊) and PHEMA (○) networks and PECH/PHEMA (37/63) (□), (43/57) (Δ), (50/50) (+), and (67/33) (*) IPNs.

modulus, i.e. stiffness. In addition, the IPN storage modulus is higher than 1000 MPa up to 40 °C. This storage modulus value is comparable with that of PECH network supported by a polyamide support [29]. Thus, IPN materials could be used from 0 to 40 °C without mechanical properties change.

The tan δ–temperature curves recorded on PECH/PHEMA IPNs and corresponding homopolymer networks are shown in Fig. 1(B). The mechanical relaxation temperatures (T_α) of single PECH and PHEMA networks occur at 10 and 119 °C, respectively. All the IPNs show a main mechanical α-relaxation characterized by one tan δ peak detected at intermediate temperature in between those of the two single networks. This T_α temperature depends on the IPN composition. For example, PECH/PHEMA (67/33) IPN shows a mechanical relaxation at 77 °C, while the α-relaxation of PECH/PHEMA (50/50), (37/63), (43/57) IPNs occur at 84, 88, and 93 °C, respectively. Thus, the higher the PHEMA network proportion in the IPN, the higher the relaxation temperature T_α is. The presence of a main mechanical relaxation temperature displays a satisfactory interpenetration degree of both networks inside the IPN architecture.

The thermal stabilities of the IPN membranes were evaluated by TGA measurements. Fig. 2 shows the thermograms recorded on single PECH and PHEMA networks and on IPNs containing different PECH weight compositions.

The main weight loss of the PECH network starts at 240 °C up to 320 °C. This thermal degradation in a single step has been associated with the loss of chlorine radicals and production of HCl [43]. This result is similar to that obtained by Stoica et al. [29]. The single PHEMA network presents a one-step degradation starting at 330 °C,

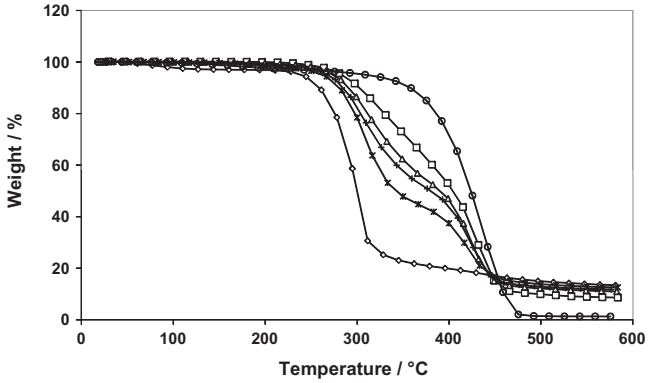

Fig. 2. TGA thermograms recorded on single PECH (◊) and PHEMA (○) networks and PECH/PHEMA (37/63) (□), (43/57) (Δ), (50/50) (+), and (67/33) (*) IPNs under argon atmosphere. Heating rate: 20 °C min^{-1}.

indicating a higher thermal stability compared with that of single PECH network.

The different IPNs show an intermediate behaviour between those of the PECH and PHEMA networks. IPNs exhibit a first thermal degradation at 250 °C which can be assigned to the PECH network degradation. The second thermal degradation is detected at 350 °C and can be assigned to that of the PHEMA network. Therefore, the degradation temperature (5 wt% weight loss) increases from 270 to 291 °C when PHEMA proportion increases from 33 to 63 wt%. The higher the PHEMA proportion, the higher the degradation temperature is. Thus the incorporation of the PHEMA network inside a PECH network increases also its thermal stability. In addition, the measurements carried out on the different IPNs deviate from the thermogravimetric curve calculated as the weighted average of those of the single PECH and PHEMA networks. Thus, PECH/PHEMA IPNs cannot be considered as a polymer blend in which the network would be independent: interactions exist between both associated networks.

These different materials are then characterized in wet state because of their use in aqueous electrolyte environment.

3.3. Loss and storage moduli, water uptake, ionic conductivity and ionic transport property measurements

After water swelling equilibrium, storage (G') and loss (G'') moduli were measured at 25 °C on membranes in the maximum swollen state at frequencies varying from 0.1 to 100 Hz. All the signals are stable on the studied frequency range (data not shown). Storage and loss moduli measured at 1 Hz are reported in Fig. 3(A).

The loss moduli of the swollen PHEMA and PECH membranes are equal to 4.2 and 0.1 kPa, respectively. The IPN loss moduli are in between those values and decrease with the PECH weight proportion. Whatever the membrane composition, the storage modulus is higher than the respective loss modulus that is characteristic of a solid viscoelastic mechanical behaviour. The G' values vary from 17.2 to 1.6 kPa with the PECH proportion ranging from 0 to 100 wt%. The mechanical stiffness is consistent with their water amount absorbed which is an important parameter related to mechanical properties and intrinsic conductivity performance. If the amount of water is too high, mechanical performance is notably impaired. On the other hand, an insufficient water amount would induce a weak ionic conductivity, since water is essential for anion mobility. The water uptake (Wu) of different PECH based IPNs was thus studied as function of the PECH proportion (Fig. 3(B)).

Single PHEMA and PECH networks show an equilibrium water uptake of 10 and 110%, respectively. Water uptake of IPNs varies linearly from 26 to 80% when the PECH weight proportion increases.

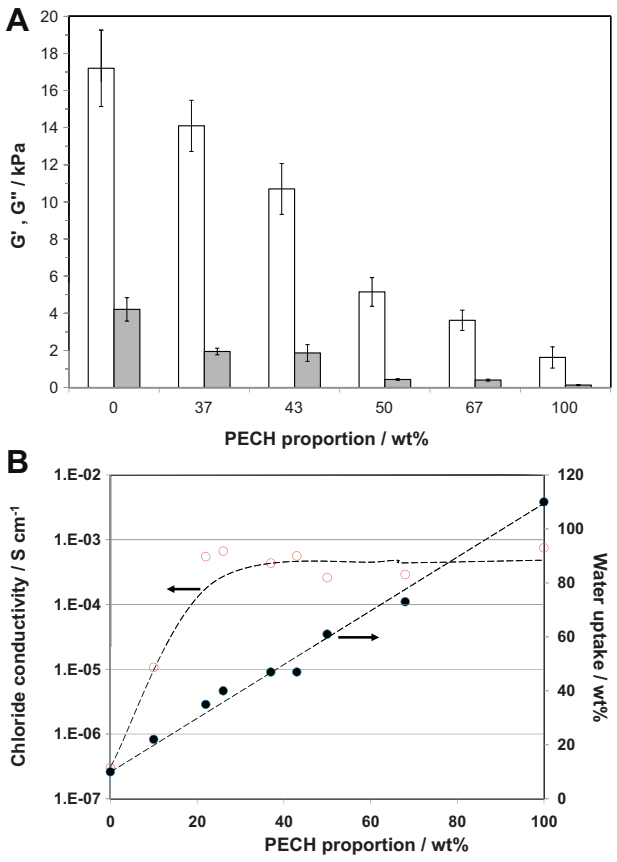

Fig. 3. (A) Storage (G', white bar) and loss (G'', grey bar) moduli of water swollen single PECH and PHEMA networks and PECH/PHEMA (37/63), (43/57), (50/50), and (67/33) IPNs. (B) Water uptake (●) and chloride conductivity (○) of the PECH based IPNs as a function of the PECH weight proportion. $T = 20\,^{\circ}C$.

Thus, the total water amount in swollen IPN corresponds to about the weight average which can be absorbed by each network separately.

Simultaneously, the anionic conductivity values of the single PECH and PHEMA networks and of IPNs with various PECH weight proportions were measured (Fig. 3(B)). As expected, the neutral single PHEMA network is not an anionic conducting material ($\sigma = 3 \times 10^{-7}\,S\,cm^{-1}$) and the anionic conductivity of the single PECH network in the fully hydrated state is $7 \times 10^{-4}\,S\,cm^{-1}$ in chloride form (Wu = 110%). As a result, the ionic conductivities of the PECH/PHEMA IPNs depend on the PECH weight proportion. The conductivity is lower than $1 \times 10^{-4}\,S\,cm^{-1}$ when the PECH proportion is lower than 20 wt% which corresponds to a percolation threshold value. For higher PECH proportions, all the IPNs have a chloride conductivity value in the range of $1–3 \times 10^{-4}\,S\,cm^{-1}$ not depending on the IPN composition. However, these anionic conductivity values are ten times lower than the highest values generally reported for quaternized polymer membranes. Indeed, Varcoe et al. reported a conductivity of $2–3 \times 10^{-3}\,S\,cm^{-1}$ for quaternized poly (vinylbenzyl chloride) membrane [11,43]. Anionic conductivities of $9.7 \times 10^{-3}\,S\,cm^{-1}$ and $7.1 \times 10^{-3}\,S\,cm^{-1}$ were also reported for cross-linked quaternized poly(vinyl alcohol) (3.9% substitution degree at 70 °C) [44] and chitosan membranes (36% substitution degree at 25 °C) [14], respectively. The difference between the conductivity values of PECH-based IPN and other cross-linked quaternized polymer membranes can be explained by a lower water swelling ratio of the IPNs. For example, the cross-linked quaternized poly(vinyl alcohol) shows a water uptake of 240% instead of less than 100% for the PECH-based materials. For the AEMA application, it is important that the ionic conductivity is as high as possible in order to limit the polarization of the IPN modified air electrode but with a controlled and limited water uptake to keep correct mechanical properties.

The IPN membranes will be in contact with lithium hydroxide electrolyte in the half-cell, which means that chloride ions will be exchanged by the hydroxide ones from the electrolyte at the beginning of the electrochemical measurements. The Cl^- ions from membranes are thus exchanged by OH^- ions. The OH^- conductivities were measured (Table 2) and show about three or four times higher values than the chloride conductivity values. These conductivity results are in agreement with the difference of mobility of hydroxide and chloride ions.

Finally, when the IPNs are swollen with potassium hydroxide solution, all the swollen materials show a similar conductivity of $10^{-2}\,S\,cm^{-1}$, which is comparable with values reported for polymer membranes swollen with such electrolyte solution. For example, chitosan network cross-linked with glutaraldehyde and containing potassium hydroxide shows ionic conductivities of 10^{-6} and $10^{-2}\,S\,cm^{-1}$ in the dry and hydrated states, respectively [45].

The transport numbers of anion (t^-) of PECH/PHEMA IPNs were also measured (Table 2) and it delivers information on the ionic selectivity of the sample under electric field. The single PECH network shows a hydroxide transport number of 0.95 which is in agreement with the transport number values generally reported for PECH-based membranes [25]. Whereas the PECH network can be considered as selective towards cations, the PHEMA network is not selective ($t^- = 0.64$). However, when the PHEMA network is included into the IPN architecture, it does not induce a significant decrease in the IPN selectivity compared with that of PECH network. Indeed, the PECH/PHEMA IPNs are characterized by a transport number value ranging from 0.84 to 0.90 indicating that the ionic transport inside the IPN is mainly anionic. Thus, the alkaline counter ions (K^+, Li^+, Na^+, etc.) of the electrolytic solution would be blocked by the IPN membrane assembled on the air electrode surface and the carbonate formation in the triple boundary phase of the air electrode would be limited.

3.4. Electrochemical properties

First, the performances of the bare commercial electrode are measured as reference in a half cell assembly. The commercial Electric Fuel® electrodes consist in cobalt based catalyzed carbon combined with a porous polytetrafluorethylene (PTFE) film on a metal mesh. In order to study the mechanism of carbon

Table 2
Intrinsic and hydroxide ionic conductivities, and anionic transport number of single PECH, PHEMA networks and IPNs. $T = 20\,^{\circ}C$.

PECH/PHEMA IPN (w/w)	σ (Cl^-) ($mS\,cm^{-1}$)	σ (OH^-) ($mS\,cm^{-1}$)	OH^- transport number
0/100 (PHEMA network)	–	–	0.64
(37/63)	0.11	0.43	0.84
(43/57)	0.18	0.66	0.86
(50/50)	0.26	0.83	0.87
(67/33)	0.29	1.11	0.90
100/0 (PECH network)	0.75	1.50	0.95

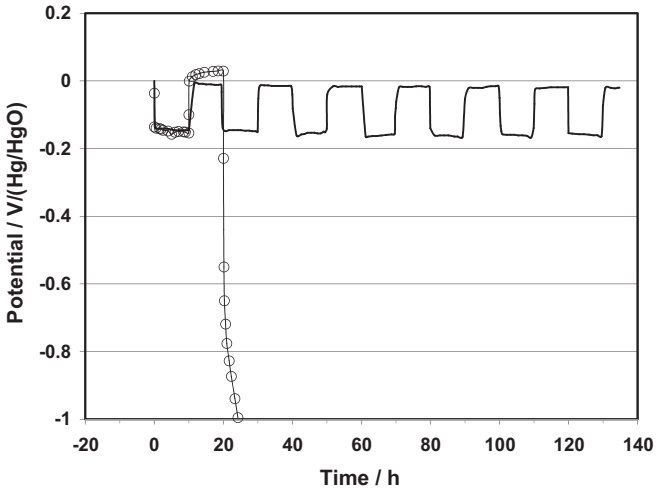

Fig. 4. Potential–time curves of a bare electrode supplied with (○) untreated and (—) treated air. Cycle: $-10\,mA\,cm^{-2}$ for 10 h and OCV for 10 h. Electrolyte: 5 mol L^{-1} LiOH. Room temperature and atmospheric pressure. Reference electrode: Hg/HgO.

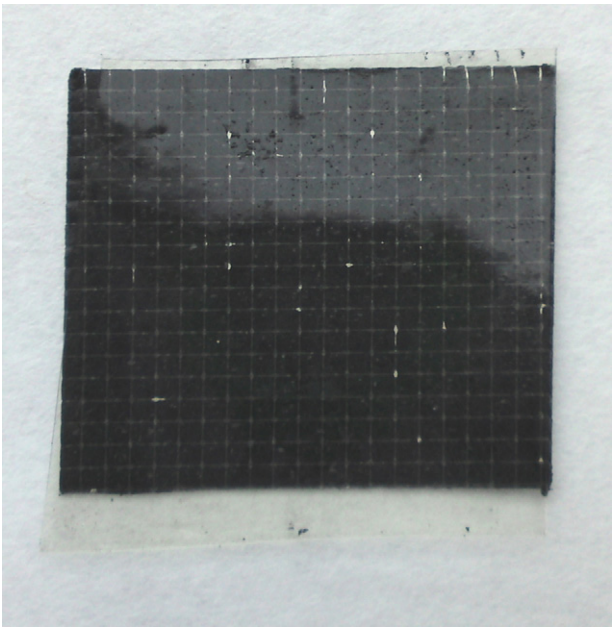

Fig. 5. Photograph of an air electrode/IPN (67/33) membrane assembly.

dioxide poisoning in alkaline media, the stability of air electrodes are studied in a 5 mol L^{-1} LiOH aqueous electrolyte. The air electrode is put into operation with ambient air or with treated air for comparison. The current density is set at $-10\,mA\,cm^{-2}$ for 10 h followed by 10 h in open circuit voltage (OCV) (Fig. 4). This cycling program is chosen to reproduce the operation of the air electrode in the bi-electrode configuration during full cell cycling [46]. This bi-electrode consists of an air electrode in combination with a secondary oxygen evolution electrode [47] and it prevents degradation of the air electrode from oxygen evolution by decoupling it during charge.

When the half-cell is supplied with untreated air, the bare electrode shows rapid degradation within 20–30 h (Fig. 4). The electrode polarization becomes very significant at the beginning of the second discharge. The bare electrode stability is thus estimated to be about 20 h. In order to confirm that the degradation electrode is mainly due to lithium carbonate formation, the same experiment has been carried out with treated air. The potential of the air electrode remains stable at 150 mV/Hg/HgO under discharge in a 5 mol L^{-1} LiOH electrolyte after more than 600 h (Fig. 4). No increase of the air electrode polarization can be detected clearly showing that the reduction of the air electrode performances is mainly due to the presence of carbon dioxide in air.

This preliminary study shows that the commercial air electrodes cannot be used in the lithium–air cell under untreated air without being protected beforehand from LiOH electrolyte. Therefore, the air electrode has been protected with different PECH based membranes.

The PECH-based membrane is assembled on air electrode surface (electrolyte side) in order to improve the chemical resistance of the electrode under these experimental conditions. The air electrode/membrane assembly is prepared by lightly pressing the wet PECH network or IPN membrane (100–150 μm) on the catalyst-coated electrode surface (Fig. 5).

First, the electrochemical stability domains of air electrode/polymer membrane assemblies were determined. The voltamperograms were recorded on the different modified electrodes in 5 mol L^{-1} LiOH solution with a 2.5 mV s^{-1} scan rate with a stainless steel plate as counter-electrode. Neither oxidation nor reduction peak was detected between 0.2 and −0.8 V/(Hg/HgO). Thus, the polymer membranes do not reduce the electrochemical stability domain of the air-electrode (result not shown).

Fig. 6 shows the polarization curves where the air-electrode is modified or not with a single PECH network or an IPN membrane (polarization curves are identical whatever the IPN composition). The polarization curves inform also on the wettability of the electrode structure in the presence of polymer membrane. The applied current densities were increased from −1 to $-100\,mA\,cm^{-2}$ and the electrode potential was measured.

The modified air electrode potentials are about −70 mV/(Hg/HgO) at current densities of $-1\,mA\,cm^{-2}$ and reach a value of −440 mV at $-50\,mA\,cm^{-2}$ indicating a similar oxygen reduction rate when the electrode is modified with PECH network or IPN. At low current densities ($\geq -5\,mA\,cm^{-2}$) both electrode potential evolutions are governed by reaction rate at the triple phase region. Therefore, the electrolyte transport towards the membrane is not restricted. At higher current densities ($<-5\,mA\,cm^{-2}$), the potentials of the modified air electrode vary linearly with the current density. This behaviour is generally associated to ohmic drop due to the ionic transport limitation towards the electrolyte and electrodes. From curves in Fig. 6, these ohmic drops can be estimated to about 5.1 and 5.2 Ω cm^2 for bare and

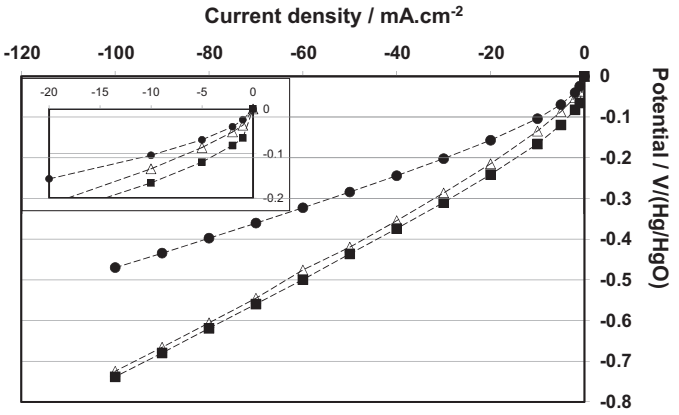

Fig. 6. Potential–current density curve recorded on a (●) bare electrode and air-electrode assembly with (Δ) PECH network or (■) PECH/PHEMA (67/33) IPN membrane. Insert: zoom at low current density. Electrolyte: 5 mol L^{-1} LiOH. Room temperature, untreated air, and atmospheric pressure. Reference electrode: Hg/HgO.

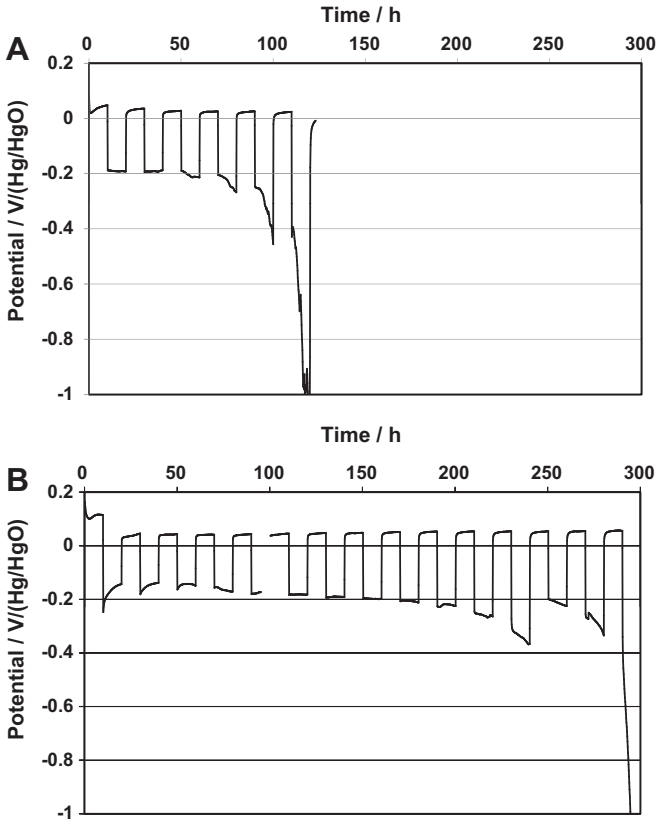

Fig. 7. Potential–time curves recorded on (A) air-electrode/PECH network and (B) air electrode/PECH/PHEMA (67/33) IPN assemblies. Cycle: OCV for 10 h and $-10\,mA\,cm^{-2}$ for 10 h. Electrolyte: $5\,mol\,L^{-1}$ LiOH. Room temperature, untreated air, and atmospheric pressure. Reference electrode: Hg/HgO.

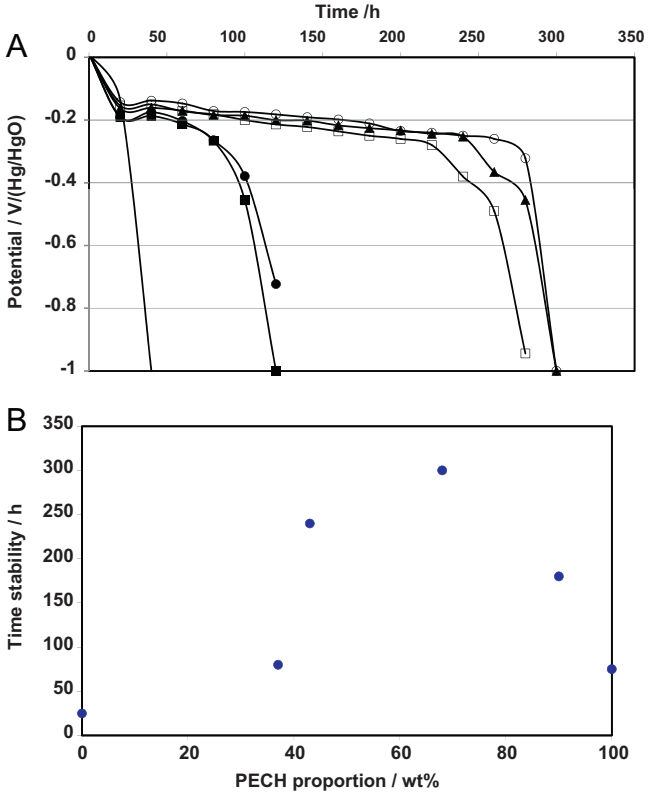

Fig. 8. (A) Potential at the discharge end–time curves recorded on (—) bare electrode, (■) air electrode/PECH network assembly, air electrode/PECH/PHEMA (●) (37/63), (□) (43/57), (○) (67/33), and (▲) (90/10) IPN assemblies. (B) Time at which the assembly potential is higher than −300 mV/(Hg/HgO) versus PECH weight proportion in the IPN. Cycle: $-10\,mA\,cm^{-2}$ for 10 h and OCV for 10 h. Electrolyte: $5\,mol\,L^{-1}$ LiOH. Room temperature, untreated air, and atmospheric pressure. Reference electrode: Hg/HgO.

modified electrodes, respectively. Thus the presence of polymer membrane (PECH network or IPN) does not induce a significant additional ohmic drop. The different polymer membranes can then be directly assembled with an air electrode without significant performance losses compared with bare electrode, especially for discharge current densities lower than $-50\,mA\,cm^{-2}$. For instance, the potential of the air electrode/IPN assembly is about 70 mV higher than the bare electrode one at $-10\,mA\,cm^{-2}$.

Finally, the stability of air-electrode/polymer membrane assemblies was studied. The half-cells were cycled in $5\,mol\,L^{-1}$ LiOH aqueous solutions at room temperature using a 10 h polarization step ($-10\,mA\,cm^{-2}$ current density) followed by 10 h at OCV to reproduce the operation of the air electrode in lithium–air battery [46]. Fig. 7 shows, as instance, the evolution of the potential as function of time of the air electrode assembled with, on the one hand, single PECH network and, on the other hand, PECH/PHEMA (67/33) IPN membrane.

The polarization–time curve recorded on air electrode/PECH network assembly (Fig. 7(A)) shows that the presence of the single PECH network membrane on the electrode increases the air electrode stability under untreated air supply. The assembly polarization keeps stable for 4 complete cycles before the air electrode polarization decreases gradually at the beginning of the fourth discharge. This result shows that an air electrode can be protected from the lithium carbonate formation in $5\,mol\,L^{-1}$ LiOH aqueous solution by applying an anion conducting/selective membrane on the electrolyte side.

The degradation process is faster than the bare air electrode one when a single PHEMA network membrane is coated on the air electrode surface (result not shown). This fast degradation is due to the additional voltage induced by this insulating material. Otherwise, the potential of an air electrode/PECH/PHEMA (67/33) IPN assembly can remain constant during more than 280 h (Fig. 7(B)). Thus, the PECH-based IPN membrane improves more than one order of magnitude the electrochemical stability of air electrode in concentrated LiOH solution compared with a bare electrode. The stability of IPN modified electrode is more than 3 times higher than that of PECH network modified electrode. This behaviour may be due to the IPN architecture which provides hydroxide conductivity together with a structural polymer able to provide mechanical stability and limited electrolyte uptake.

In order to compare the stability of the different assemblies, and more especially the effect of IPN composition, the air electrode potential at the end of each discharge is reported as function of time (Fig. 8(A)). It is clearly shown that the stability of the modified electrode depends on the IPN composition though the initial polarization at $-10\,mA\,cm^{-2}$ is similar for any IPN composition.

From Fig. 8(A), the duration corresponding to an assembly potential higher than −300 mV (Hg/HgO) (beginning of the potential drop) has been reported versus the IPN composition (Fig. 8(B)). This curve clearly shows that IPN composition has a considerable effect on the air electrode stability. The assembly is stable less than 100 h when the PECH proportion in the IPN is lower than 37 wt% or when a single PECH network is used. It seems that an optimum composition of IPN would be about 50 wt% PECH that would appear as a good compromise between swelling ratio and selectivity (transport number). Because the IPN architecture shows better mechanical properties with an electrolyte reduced swelling and without conducting property loss, this architecture seems to be particularly appropriate for use as membrane/separator in alkaline batteries.

4. Conclusion

In this work, we demonstrate that the original combination of PECH and PHEMA networks in an interpenetrating polymer network architecture could increase significantly the PECH polyelectrolyte mechanical properties while preserving a good hydroxide conductivity and anion selectivity. The air electrode modified with these IPNs shows no significant ohmic drop compared with the bare electrode. Moreover the AEMA stability in discharge mode is more than 10 times longer than that of the bare air electrode. This air electrode modification with a PECH/PHEMA IPN prevents the Li^+ ions moving from the alkaline electrolyte to the electrode, and limits the lithium carbonate formation. The carbon dioxide role on the electrode stability has been clearly demonstrated by carrying out similar measurements under treated air. Thus the degradation phenomena (folding, carbonate formation) of the air electrode were drastically reduced by the original IPN membrane presence on the electrode. The optimization of the membrane–electrode contact and the study of ageing mechanism of the assembly are in progress, this should allow a further increase of the lifetime of air electrodes in concentrated alkaline aqueous solutions.

Acknowledgments

This work is sponsored by the *Agence Nationale de la Recherche* (*ANR*) of France (ANR-07-Stock-E-LIO-06 and ANR-10-Stock-E-LIO2). The authors would like to thank Drs. Philippe Stevens, Gwenaelle Toussaint, and Christian Sarrazin for many fruitful discussions.

References

[1] G.F. McLean, T. Niet, S. Prince-Richard, N. Djilali, Int. J. Hydrogen Energy 27 (2002) 507–526.
[2] A.V. Tripkovic, K.D. Popovic, B.N. Grgur, B. Blizanac, P.N. Ross, N.M. Markovic, Electrochim. Acta 47 (2002) 3707–3714.
[3] G.J.K. Acres, J.C. Frost, G.A. Hards, R.J. Potter, T.R. Ralph, D. Thompsett, G.T. Burstein, G.J. Hutchings, Catal. Today 38 (1997) 393–400.
[4] H.S. Wroblowa, Y.-C. Pan, G. Razumney, J. Electroanal. Chem. Interfacial Electrochem. 69 (1976) 195–201.
[5] V.S. Bagotzky, E.I. Khruscheva, M.R. Tarasevich, N.A. Shumilova, J. Power Sources 8 (1982) 301–309.
[6] D.A. Scherson, S.L. Gupta, C. Fierro, E. Yeager, M. Kordesch, J. Eldridge, R. Hoffman, Electrochim. Acta 28 (1983) 1205–1209.
[7] Y. Kiros, O. Lindström, T. Kaimakis, J. Power Sources 45 (1993) 219–227.
[8] M. Cifrain, K.V. Kordesch, J. Power Sources 127 (2004) 234–242.
[9] E. Gülzow, J. Power Sources 61 (1996) 99–104.
[10] T. Burchardt, J. Power Sources 135 (2004) 192–197.
[11] R.C.T. Slade, J.R. Varcoe, Solid State Ionics 176 (2005) 585–597.
[12] J.R. Varcoe, R.C.T. Slade, Electrochem. Commun. 8 (2006) 839–843.
[13] Y.-L. Choi, J.-M. Park, K.-H. Yeon, S.-H. Moon, J. Membr. Sci. 250 (2005) 295–304.
[14] Y. Wan, B. Peppley, K.A.M. Creber, V.T. Bui, E. Halliop, J. Power Sources 185 (2008) 183–187.
[15] Y. Wan, K.A.M. Creber, B. Peppley, V.T. Bui, J. Membr. Sci. 284 (2006) 331–338.
[16] J. Fang, P.K. Shen, J. Membr. Sci. 285 (2006) 317–322.
[17] J.R. Varcoe, R.C.T. Slade, Fuel Cells 5 (2005) 187–200.
[18] L. Li, Y. Wang, J. Membr. Sci. 262 (2005) 1–4.
[19] E.L. Dewi, K. Oyaizu, H. Nishide, E. Tsuchida, J. Power Sources 115 (2003) 149–152.
[20] X. Yan, G. He, S. Gu, X. Wu, L. Du, H. Zhang, J. Membr. Sci. 375 (2011) 204–211.
[21] F. Yi, X. Yang, Y. Li, Polym. Adv. Technol. 10 (1999) 473–475.
[22] N. Vassal, E. Salmon, J.F. Fauvarque, Electrochim. Acta 45 (2000) 1527–1532.
[23] F. Tronel, L. Gautier, T. Brincourt, J. Phys. IV 12 (2002) 39–47.
[24] E. Agel, J. Bouet, J.F. Fauvarque, H. Yassir, Ann. Chim. Sci. Mater. 26 (2001) 59–68.
[25] E. Agel, J. Bouet, J.F. Fauvarque, J. Power Sources 101 (2001) 267–274.
[26] B. Bauer, H. Strathmann, F. Effenberger, Desalination 79 (1990) 125–144.
[27] C. Iojoiu, F. Chabert, M. Marechal, N.El. Kissi, J. Guindet, J.-Y. Sanchez, J. Power Sources 153 (2006) 198–209.
[28] C. Sollogoub, A. Guinault, M. Bennjima, L. Akrour, J.F. Fauvaque, L. Ogier, J. Membr. Sci. 335 (2009) 37–42.
[29] D. Stoica, L. Ogier, L. Akrour, F. Alloin, J.F. Fauvarque, Electrochim. Acta 53 (2007) 1596–1603.
[30] L.H. Sperling, V. Mishra, in: S.C. Kim, L.H. Sperling (Eds.), IPNs Around The World: Science and Engineering, Wiley, New York, 1997, pp. 1–25.
[31] L.H. Sperling, in: L.H. Sperling, D. Klempner, L.A. Utracki (Eds.), Advances in Chemistry Series, vol. 239, American Chemical Society, Washington, DC, 1994, pp. 3–38.
[32] M.S. El-Assar, R. Hu, V.L. Dimonie, L.H. Sperling, Colloids Surf. A: Physicochem. Eng. Aspects 153 (1999) 241–253.
[33] Y.H. Bae, T. Okanao, S.W. Kim, Macromol. Chem. Rapid Commun. 9 (1988) 185–189.
[34] Z. Maolin, H. Hongfei, F. Yoshii, K. Makuuchi, Radiat. Phys. Chem. 57 (2000) 459–464.
[35] L. Xuequan, Z. Maolin, L. Jianping, H. Hongfei, Radiat. Phys. Chem. 57 (2000) 477–481.
[36] L. Chikh, V. Delhorbe, O. Fichet, J. Membr. Sci. 368 (2011) 1–17.
[37] X. Han, B. Chen, F. Guo, in: S.C. Kim, L.H. Sperling (Eds.), IPNs Around The World, Wiley, New York, 1997, 241 pp.
[38] X. Han, B. Chen, F. Guo, Polym. Adv. Technol. 7 (1996) 315–322.
[39] Q. Chen, H. Ge, D. Chen, X. He, X. Yu, J. Appl. Polym. Sci. 54 (1994) 1191–1197.
[40] A.J. Bard, L.R. Faulkner, Electrochemical Methods: Fundamentals and Applications, 2nd ed., Wiley, New York, 2001 (Chapter 2).
[41] The CRC Handbook of Chemistry and Physics, 2003–2004.
[42] G. Goulart Silva, N.H.T. Lemes, C.N. Polo da Fonseca, M.A. De Paoli, Solid State Ionics 93 (1996) 105–116.
[43] J.R. Varcoe, R.C.T. Slade, E.L.H. Yee, S.D. Poynton, D.J. Driscoll, J. Power Sources 173 (2007) 194–199.
[44] Y. Xiong, J. Fang, Q.H. Zeng, Q.L. Liu, J. Membr. Sci. 311 (2008) 319–325.
[45] Y. Wan, B. Peppley, K.A.M. Creber, V.T. Bui, E. Halliop, J. Power Sources 162 (2006) 105–113.
[46] P. Stevens, G. Toussaint, G. Caillon, P. Viaud, P. Vinatier, C. Cantau, O. Fichet, C. Sarrazin, M. Mallouki, Electrochem. Soc. Trans. 28 (2010) 1–12.
[47] G. Toussaint, P. Stevens, L. Akrour, R. Rouget, F. Fourgeot, Electrochem. Soc. Trans. 28 (2010) 25–32.